

## Current Topics of Microwave EMI Antennas and Measurements

著者	Sugiura Akira, Kuwabara Nobuo, Iwasaki Takashi
journal or publication title	IEICE Transactions on Communications
volume	E80-B
number	5
page range	653-662
year	1997-05-25
URL	<a href="http://hdl.handle.net/10228/00008492">http://hdl.handle.net/10228/00008492</a>

INVITED PAPER *Special Issue on EMC/EMI Problems in Microwave Frequency Range*

# Current Topics of Microwave EMI Antennas and Measurements

Akira SUGIURA<sup>†</sup>, Nobuo KUWABARA<sup>††</sup>, and Takashi IWASAKI<sup>†††</sup>, *Members*

**SUMMARY** This paper reviews recent developments in small-sized broadband antennas for EMI measurements, especially in the microwave frequency region. Transient EMI measurements are also discussed by introducing complex antenna factors and conversion of frequency-domain data into time-domain data. This paper also focuses on considerable improvements achieved in calibration techniques for conventional EMI antennas in VHF/UHF bands.

**key words:** EMI measurement, antenna calibration, dipole antennas, antenna factor

## 1. Introduction

Recent proliferation of portable telephones has rapidly increased the potential need for measuring and controlling radio interference produced by electronic equipment, especially in the microwave frequency region. This trend has been much accelerated by the increasing clock frequencies of digital equipment. Such equipment usually generates broadband electromagnetic disturbances which, in many cases, contain very sharp pulses. Therefore, specially designed broadband antennas are required for measurements, and their characteristics have to be precisely determined not only in the frequency domain but also in the time domain.

In the microwave frequency range, many different types of antennas are used for measuring electromagnetic disturbances (traditionally called electromagnetic interference, or EMI) generated by radio transmitters and electronic equipment. These antennas may be classified into two categories depending on antenna size and characteristics. One category is for antennas on the order of half a wavelength and includes most conventional antennas which are widely used in EMI measurements related to equipment authorization. This type of antenna usually has good sensitivity. Antennas in the other category are smaller, have a broadband response, and are suitable for RF pulse measurements, but they have poor sensitivity. As a result, different calibration methods that take account of these features have been developed for each antenna

category.

In EMI measurements, the performance of a measuring antenna is primarily characterized in terms of the antenna factor, which is defined as the ratio of the electrical field strength  $E$  of an incident field to voltage  $V$  induced at the input of a connected measuring receiver, that is,  $AF = E/V$ . Using the antenna factor, the field strength of RF emission can be evaluated from a meter reading indicated by a measuring receiver. Hence, the antenna factor of the antenna used has to be accurately determined to achieve good reproducibility in EMI measurements, especially in measurements related to authorization of electronic equipment. Recently, intensive investigations have been made on antenna calibration, resulting in great improvements in conventional methods.

The present paper reviews developments in small broadband antennas and explains sophisticated techniques for measuring transient EM disturbances in terms of complex antenna factors. In addition, recent improvements in calibration techniques for conventional EMI antennas are summarized in this paper.

## 2. Broadband Antennas

### 2.1 Microwave Sensors and Antennas

Measuring electric field is important in studying electromagnetic compatibility (EMC) in the microwave frequency range. There are many antennas and sensors for making these measurements. Examples of their operating frequency ranges and antenna factors are

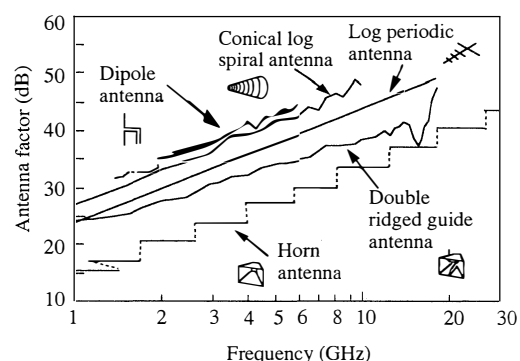


**Fig. 1** Examples of antennas and their antenna factors used for EMC measurement in the microwave frequency region.

Manuscript received January 16, 1997.

<sup>†</sup> The author is with Communications Research Laboratory, Koganei-shi, 184 Japan.

<sup>††</sup> The author is with NTT Multimedia Network Laboratory, Musashino-shi, 180 Japan.

<sup>†††</sup> The author is with University of Electro-Communications, Chofu-shi, 182 Japan.

summarized in Fig. 1. The dipole antenna, the most practical, is used for frequencies up to 6 GHz. The log-periodic dipole array antenna and the double-ridged-guide antenna exhibit linear polarization and operate from 1 GHz to 18 GHz. The conical log spiral antenna has circular polarization and operates from 1 GHz to 10 GHz. The horn antenna is also used for EMC measurement and as the standard for antenna calibration. The antenna factors of these antennas increase in proportion to the frequency. This means that it is difficult to achieve high sensitivity at high frequencies. These antennas have recently been used to cope with the progress in mobile communications and the increase in CPU clock frequency. On the other hand, other antennas and sensors have been developed for use in EMC measurement above 1 GHz. This chapter describes the broadband antennas and sensors which have recently been developed for the microwave frequency range.

## 2.2 Small Dipole Antenna

Sensors with a small dipole antenna are used to measure the electric field strength and the performance of the EMC measurement facilities [1], [2]. The basic configuration of the sensor is illustrated in Fig. 2. The

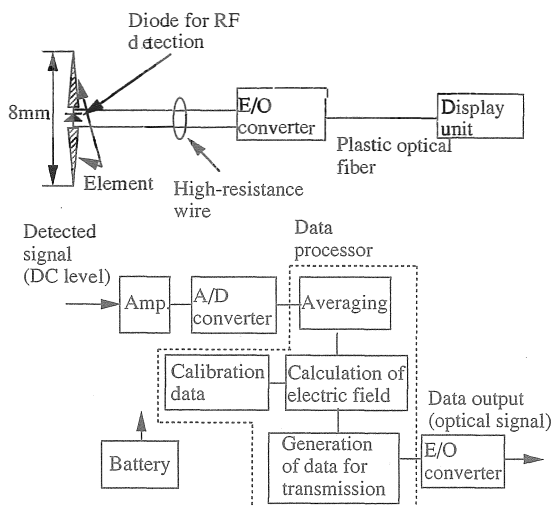


Fig. 2 Configuration of a sensor using a small dipole antenna.

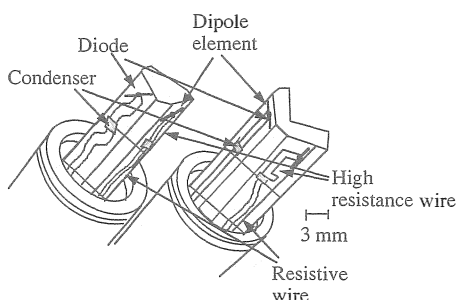


Fig. 3 Example of a sensor using a small dipole antenna.

diode converts the received electric field strength to a potential level, and a high-resistance wire reduces the influence of the cable connecting the sensor element to the level meter. The meter is constructed with an E/O converter and a display unit because the sensor is usually placed in a strong electric field. The electric field strength is calculated from the measured potential levels. Three elements are placed in orthogonal directions and used to measure the power density. A sensor with an 8.5 mm long dipole operates from 100 kHz to 18 GHz and its dynamic range is from 1 V/m to 1600 V/m [2]. A recently developed application of the sensor is measuring the specific absorption ratio (SAR) distribution [3]. The configuration of the sensors is illustrated in Fig. 3. Two types of sensors, triangular and rectangular, have been developed. These sensors have 3-mm long dipoles and operate at over 3 GHz with a dynamic range of from 1 mW/g to 100 mW/g. Small dipole antennas which can improve space resolution and operation frequency will be developed for application to EMC study in future.

## 2.3 Electromagnetic Energy Measurement Using Temperature Change

The measurement of electromagnetic energy is necessary to estimate the electric field distribution and the SAR distribution. When electromagnetic energy is absorbed by a material, the temperature of the material increases. Thus, the electromagnetic energy can be evaluated by measuring the increase in temperature. An electromagnetic energy sensor has been developed to use an optical temperature sensor [4] and the Phantom [5]. The configuration of this sensor, which uses a pair of optical temperature sensors [4], is illustrated in Fig. 4. One optical temperature sensor measures the temperature increase produced by incident RF energy, and the other measures the ambient temperature. The electromagnetic energy absorbed is calculated from the temperature difference between these sensors. This type of electromagnetic energy sensor can be easily miniaturized. A sensor of 5 mm in diameter and 13 mm long has been developed. This type of electromagnetic energy sensor is expected to be used in studies of human hazards and hyperthermia.

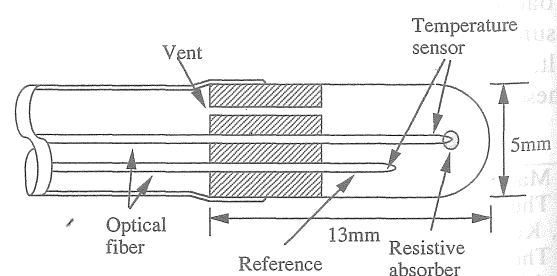


Fig. 4 Configuration of a sensor using a fiber optic temperature sensor.

2.4 Antennas with E/O and O/E Converters

The cable connecting the antenna element to the level meter can affect the measurement accuracy of the electric field strength. One approach that has been studied is to replace the coaxial cable with an optical fiber cable. The basic configurations of antennas using an optical fiber are illustrated in Fig. 5. The receiving antenna converts the received signal to an optical signal using an electrical-to-optical (E/O) converter. An optical-to-electrical converter (O/E) in the transmitting antenna then converts the optical signal to an electrical signal and radiates it into space. An example of a radiator using an O/E converter is illustrated in Fig. 6 [6]. The antenna can operate at up to 3.1 GHz and the maximum feeding RF power is 0 dBm [7]. Sensors with an E/O converter have also been proposed, and a loop antenna whose dimensions are 57\*57\*13 mm operates at up to 2 GHz [8]. The loss of a coaxial cable increases in proportion to frequency, and it influences the design of radio systems in the microwave frequency range. In contrast to this, an optical fiber, which has the extremely low insertion loss of less

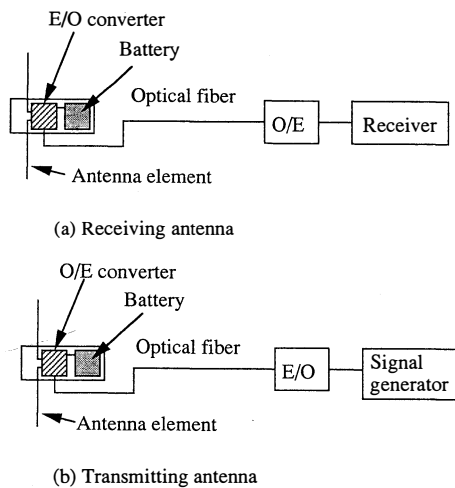


Fig. 5 Configuration of an antenna using electro-optical (E/O) and optical-electro (O/E) converters.

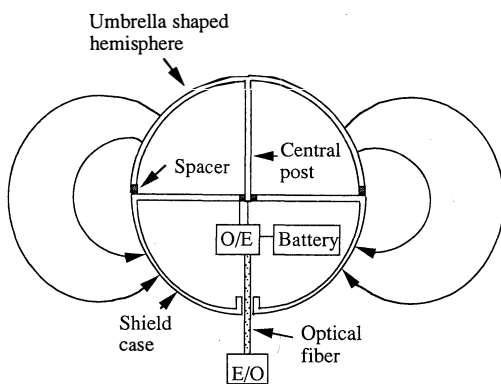


Fig. 6 Example of a spherical dipole transmission antenna.

than 1 dB/km, can be used in a remote control system [9]. Other applications, such as a standard RF source for calibrating antennas and measuring the shielding effect of a cabinet, are studied [7].

2.5 Electric Field Sensor Using Optical Modulator

Optical modulators can operate above 10 GHz. They have been studied for use as the E/O converter of an antenna in the microwave frequency range. The sensitivity and maximum operating frequency of various sensors with optical modulators are summarized in Fig. 7. A sensor with an optical modulator composed of bulk LiNbO<sub>3</sub> crystals was proposed in 1980 [10], [11]. Before 1994, efforts to improve sensor sensitivity focused on increasing the half-wave voltage of the optical modulator [12] and decreasing the input capacitance of the modulator [13]. A method of tuning the optical bias angle was also proposed [14]. Recently, ways of increasing the maximum operating frequency have been studied to allow use in the microwave frequency range [15]. An example of the configuration of an electric field sensor with an optical modulator is illustrated in Fig. 8 [15]. This sensor has an optical source, a polarization maintaining fiber, an optical modulator, a sensor element, a single mode optical fiber, and a photodetector. A 10-mm long dipole element is used as the sensor element. When the

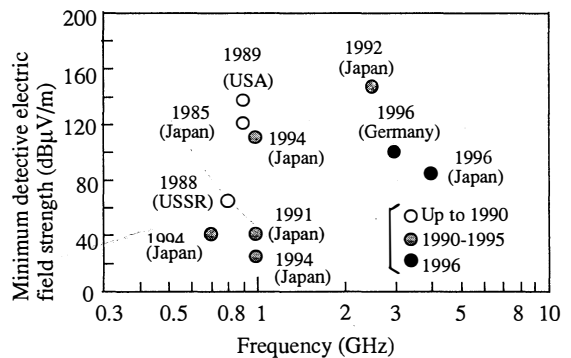


Fig. 7 Sensitivity and bandwidth of optical modulator type electric field sensors.

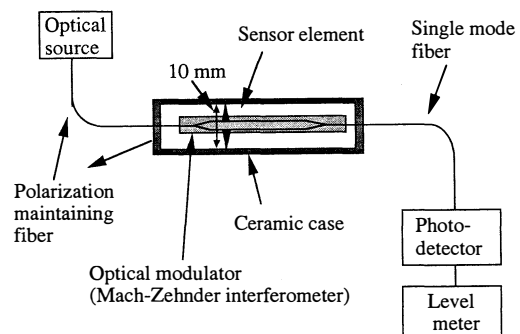


Fig. 8 Configuration of an electric field sensor using a Mach-Zehnder interferometer.

sensor element is placed in an electric field, a voltage appears at the sensor element. The optical modulator changes the optical power with this voltage variation. The electric field strength can be estimated by measuring the modulated optical signal level. The sensitivity of the sensor is almost constant from 1 GHz to 4.3 GHz. In addition, the use of a small element improves the spacial resolution of measuring the electric field strength distribution [14]. It is useful for measuring the electric field distribution near an antenna of a wireless telephone, such as GSM or PDC phones.

Another measuring method based on the electro-optic effect has been developed to measure signals on high speed LSI [16]. A temporal resolution of 20 ps and a spacial resolution of 2 mm were obtained. The sensitivity of sensors using optical modulators is almost independent of frequency. This means that this type of sensor is useful for measuring the electromagnetic pulses. The improvement of the sensitivity and operating frequency range will be a future problem to be solved before using it in the measurement of electromagnetic pulses.

### 3. Measurements of Transient Electromagnetic Fields

#### 3.1 Sensors and the Characteristics

Transient electromagnetic fields caused by electrostatic discharges (ESD) or pulse electromagnetic waves generated by electro-optic devices have very wide bandwidths. Their spectrums extend over the microwave region or even the millimeter wave region [17], [18]. In the near fields of such electromagnetic sources, both electric and magnetic waveform measurements are desired, because the two waveforms are different. Several kinds of sensors with antennas have been used for measuring such high-speed transient electric and magnetic fields [19], [20]. The usual way to obtain a wide-band sensor is to make the antenna small.

Baum classified the electric and magnetic sensors, and showed the simple equivalent circuits of small antennas as shown in Fig. 9 and Fig. 10, where  $l_{eq}$  is the antenna equivalent length and  $A_{eq}$  is the antenna equivalent area [21]. A short dipole antenna and a small loop antenna can be used to detect electric field and magnetic field, respectively. These equivalent circuits show that the output waveforms are different from those of incident fields due to the antenna characteristics. In general, the capacitance  $C$  and the inductance  $L$  depend on frequency. Moreover, antennas usually have attachment circuits to couple with external instruments. Therefore, the real waveforms of the fields should be reconstructed from the sensor output considering the characteristics of the antennas and attachment circuits. The reconstruction can be made in the time domain or in the frequency domain [22].

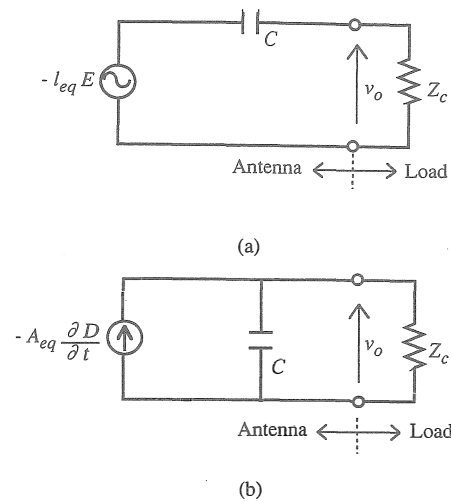


Fig. 9 Equivalent circuits of small dipole antenna. (a) Thevenin equivalent circuit. (b) Norton equivalent circuit.

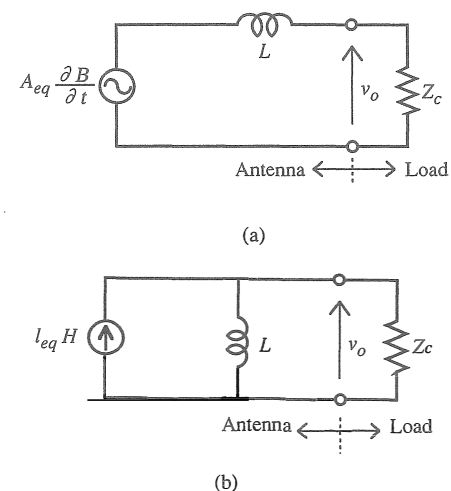


Fig. 10 Equivalent circuits of small loop antenna. (a) Thevenin equivalent circuit. (b) Norton equivalent circuit.

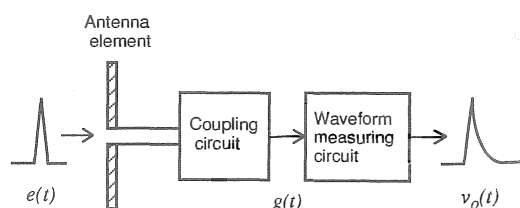


Fig. 11 Configuration of a typical electric field sensor.

#### 3.2 Reconstruction in the Time Domain

Figure 11 shows the configuration of a typical electric field sensor consisting of an antenna element, a coupling circuit, and a waveform measuring circuit. If the response of this system is linear and time-invariant, the

output voltage of this sensor,  $\nu_0(t)$ , may be expressed as the convolution integral,

$$\nu_0(t) = \int_{-\infty}^{\infty} e(t)g(t-\tau) d\tau, \quad (1)$$

where  $e(t)$  is the incident electric field and  $g(t)$  is the impulse response of this sensor system. If the impulse response  $g(t)$  can be measured, the incident electric field  $e(t)$  can be reconstructed by the discrete deconvolution in the time domain. For the incident magnetic field  $h(t)$ , the measurement system and the convolution relation are respectively the same as Fig. 11 and Eq. (1).

To measure the impulse response, an electrical impulse of the incident field (delta-function-like field) is necessary. Since an electrical transient field with a microwave bandwidth is to be measured, a pico-second order impulse field is required. However, it is difficult to make such an incident field with a sufficient accuracy. Shen measured the output waveforms of several sensors to an electromagnetic impulse with a width of 66 ps [23]. However, the measurement method and system of the incident impulse itself was not shown. So far, the time domain deconvolution of transient or pulse electromagnetic fields with a microwave bandwidth has not been reported.

Another approach is to calculate the time domain characteristics of a sensor theoretically. Middelkoop proposed the following magnetic sensor factor for the type of sensor shown in Fig. 10(b) [24].

$$F_h(t) = h(t)/\nu_0(t). \quad [\text{A/m/V}] \quad (2)$$

Here,  $h(t)$  is the incident magnetic field. The electric sensor factor is expressed as,

$$F_e(t) = e(t) / \int_{\tau_i}^{\infty} \nu_0(t) dt \quad [\text{V/m/V}] \quad (3)$$

for the type of sensor shown in Fig. 9(b), where  $\tau_i$  is an integration time constant. A closed circular loop for the magnetic sensor and a hollow spherical dipole for the electric sensor were constructed. Their sensor factors were calculated using the dimensions of the physical structures. This method, however, can be hardly applied to the microwave bandwidth pulses, because the characteristics of the coupling circuit and the waveform measuring circuit shown in Fig. 11 are not considered.

### 3.3 Reconstruction in the Frequency Domain

Using the convolution theorem, Eq. (1) can be written in the frequency domain as,

$$V_0(\omega) = E(\omega) G(\omega), \quad (4)$$

where  $\omega$  is angular frequency.  $V_0(\omega)$ ,  $E(\omega)$ , and  $G(\omega)$  are the Fourier transforms of  $\nu_0(t)$ ,  $e(t)$ , and  $g(t)$ , respectively. All the functions,  $V_0(\omega)$ ,  $E(\omega)$ , and

$G(\omega)$ , have complex values. Using the transfer function  $G(\omega)$ , the incident electric field can be reconstructed in the frequency domain,

$$e(t) = \mathcal{F}^{-1}\{V_0(\omega)/G(\omega)\}, \quad (5)$$

where  $\mathcal{F}^{-1}\{\dots\}$  denotes the inverse Fourier transform.

Kanda reported pioneering work on waveform reconstruction in the frequency domain [25], [26]. The effective length and the driving-point impedance of a resistively loaded dipole antenna were calculated by the moment method. The transfer function was derived from the characteristics and the load impedance. The time domain responses were obtained using the fast Fourier transform (FFT).

Yokoshima defined the inverse of the transfer function as the complex antenna factor (CAF) [27]. The conventional scalar antenna factor used in EMI measurements is the magnitude of the CAF. The CAF can be determined by the modified 3-antenna method in which transmission S-parameters, instead of scalar site attenuation, are measured by using a microwave network analyzer. The CAF includes the characteristics of the coupling circuit shown in Fig. 11, and can be determined experimentally. Therefore, reconstruction by the measured CAF method is applicable to the waveform measurements using antennas with a coupling circuit including a balun (balanced-unbalanced transformer) which is difficult to analyze theoretically.

Ishigami measured the transient electromagnetic fields of a small gap discharge between an electrode and the ground plane using the following reconstruction algorithm [28], [29],

$$\begin{aligned} e(t) &= \int_0^t \frac{de(t)}{dt} dt \\ &= \int_0^t \mathcal{F}^{-1}\left\{j\omega F_c(\omega) \frac{\mathcal{F}\{\nu_0(t)\}}{S_{21}(\omega)}\right\} dt \end{aligned} \quad (6)$$

where  $\mathcal{F}\{\dots\}$  denotes the Fourier transform,  $F_c(\omega)$  is the CAF,  $\nu_0(t)$  is the output voltage of the coupling circuit, and  $S_{21}(\omega)$  is the transmission S-parameter of the waveform measuring circuit shown in Fig. 11. In the above equation, the term of  $j\omega$  carries out differentiation in the frequency domain. This process is introduced to cope with the diversity of  $F_c(\omega)$  at  $\omega = 0$ . The equation for the magnetic field measurements is same as the above equation. Examples of output voltages  $\nu_0(t)$  are shown in Fig. 12, where (a) and (b) were measured by using a monopole antenna and a half-loop antenna, respectively. The reconstructed electric field from Fig. 12(a) is shown in Fig. 13(a), and the magnetic field from Fig. 12(b) is shown in Fig. 13(b), where the field strength polarities are opposite to the polarities of the voltage applied to the gap.

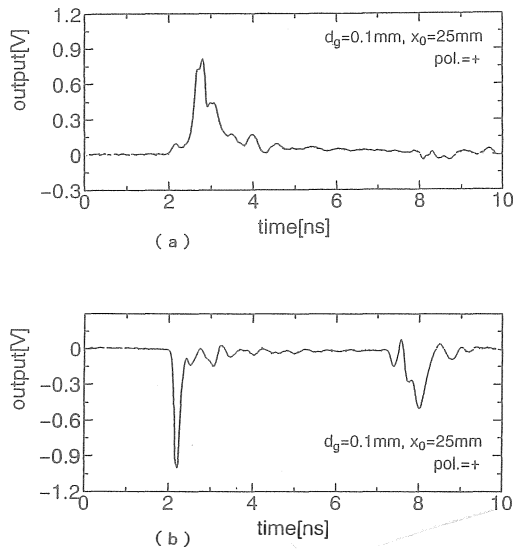


**Fig. 12** Examples of output voltage of electric and magnetic sensors.

(a) With a monopole antenna.

(b) With a half-loop antenna.

$d_g$ : gap length between the electrode and the ground plane.

$x_0$ : distance between the electrode and the sensors.

$\text{pol.}$ : polarity of the applied voltage.

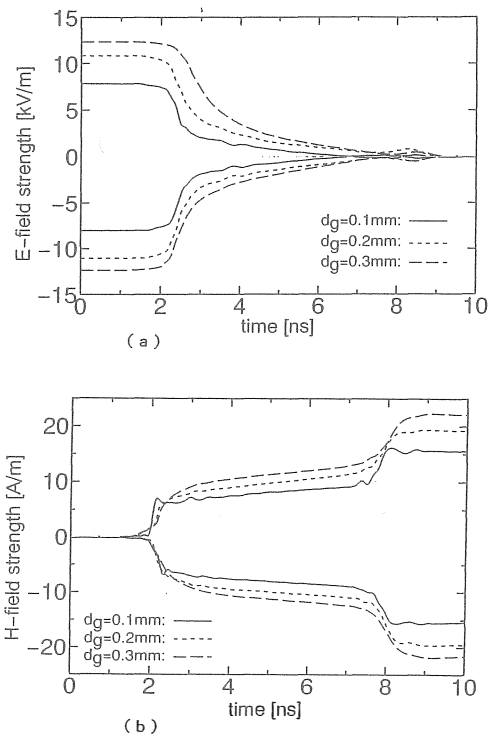


**Fig. 13** Reconstructed electric and magnetic fields.

(a) Electric field strength obtained from Fig. 12(a).

(b) Magnetic field strength obtained from Fig. 12(b).

#### 4. Calibration of EMI Antennas

Since conventional EMI antennas are as large as half a wavelength, their calibration requires an outdoor measuring site or a huge anechoic chamber. Kanda extensively reviewed the currently used calibration techniques for VHF/UHF bands [30]. One of the key technologies in calibration concerning the antenna factor is the method of determining the strength of an EM field in which the antenna under calibration (AUC) is immersed. There are two calibration techniques being employed at national standard laboratories. The Standard Antenna Method needs a specially-designed receiving antenna to determine exactly an unknown field strength from the measured RF voltage derived from the antenna. In contrast to this method, the Standard Field Method uses a standard transmitting antenna to produce an EM field at an AUC, the strength of which can be accurately evaluated by measuring the supplied power and gain of the standard antenna. With respect to antenna gain calibration, there is the Three-Antenna Method based on the Friis transmission formula. It uses two arbitrary antennas together with an AUC to determine precisely the gain of each antenna. Since a free-space environment is required, this method has been employed mostly in the frequency range above 1 GHz.

Recently, intensive studies have been made of the calibration methods of conventional EMI antennas to satisfy the demand of industry. For example, standard dipole antennas have been rigorously analyzed for use in practical antenna calibration. In addition, great improvements have taken place on the Standard Site Method for accurate antenna calibration.

##### 4.1 Standard Antenna Method

In calibration with the conventional Standard Antenna Method, a half-wave tuned dipole is normally used as a standard antenna with a high impedance shunt diode connected across the center gap of the antenna, as illustrated by Fig. 14(a). The RF open-circuit voltage induced in the dipole is measured in terms of the rectified dc voltage, which is filtered by a low-pass network and fed to a high-impedance dc voltmeter. The strength of the incident field can be determined from the measured RF open-circuit voltage multiplied by the effective length of the antenna. Therefore, the effective length is the most important parameter that needs to be theoretically evaluated.

An alternative standard antenna with a simple structure was developed by Fitzgerrell [31] and its characteristics were theoretically analyzed by Salter and Alexander [32]. It is an ordinary half-wave tuned dipole antenna as indicated by Fig. 14(b), but the connected balun is a precise coaxial hybrid network

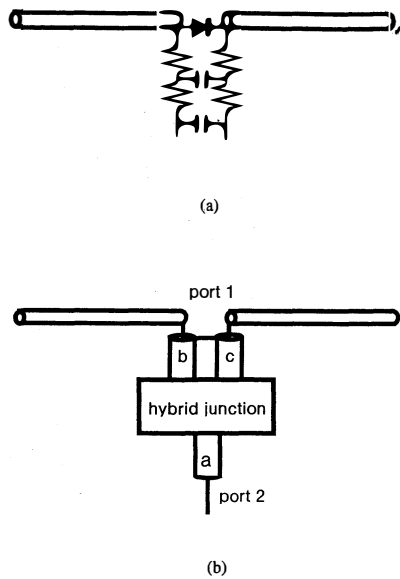


**Fig. 14** Standard dipole antennas.  
 (a) Antenna with a diode  
 (b) Antenna with a hybrid junction

freely available on the market. The balun has coaxial ports and can be removed from the antenna elements so that its characteristics can be accurately measured using a network analyzer. Hence, the electrical properties, including the antenna factor, can be calculated with sufficient accuracy for this standard antenna. The accuracy of the numerical modeling of the antenna was proved by comparing the experimental and theoretical values of transmission loss (site attenuation) between two standard antennas placed at a given height on a measuring site (test site). Alexander et al. reported that, for horizontally polarized antennas, agreement was obtained to within  $\pm 0.1$  dB in a frequency range of 30–300 MHz [33]. This deteriorated to  $\pm 0.8$  dB at 1 GHz, which is attributable to the increased ratio of the feed gap to dipole length. It was concluded that the excellent agreement proved that the antenna factors of this standard antenna were calculable to a high level of precision.

4.2 Standard Site Method

More than ten years ago, a new calibration method for VHF/UHF antennas was proposed. That method is very similar to the Three-Antenna Method, except that transmission loss measurements between two antennas are performed at the test site [34]. It postulates that the site should be of infinite extent and covered with a perfectly conducting ground plane, as illustrated in Fig. 15. Hence, the accuracy of the antenna factor obtained using this method strongly depends on the quality of the actual site. Because of this fact, the method is referred to as the Standard Site Method (SSM). The SSM is much easier to implement than

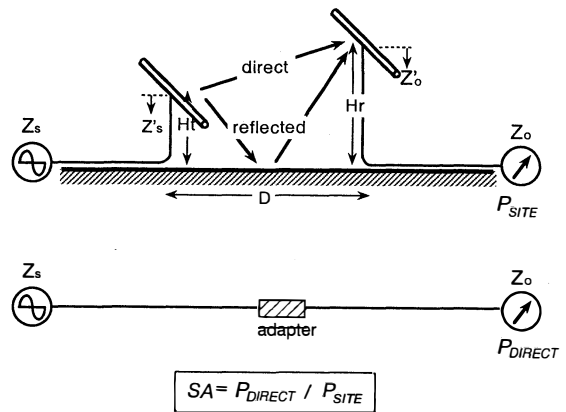


**Fig. 15** Antenna arrangement for the Standard Site Method.

the aforementioned Standard Antenna Method, because it can be performed on a conventional EMI test site without using any special antennas. Therefore, the latest version of American National Standard ANSI C63.5 features this calibration method.

Sugiura et al. did a theoretical analysis of the SSM using matrix representations and derived the fundamental expression for the site attenuation, SA, between antennas in terms of their antenna factors,  $AF'$  [35].

$$SA = \frac{|Z'_s Z'_o|}{0.0896 f_{MHz} |Z'_s + Z'_o|} \frac{AF'_1(Ht) AF'_2(Hr)}{E(D, Ht, Hr)} \quad (7)$$

This equation corresponds to the Friis transmission formula used in the free-space Three-Antenna Method. The source and receiver impedances are denoted by  $Z_s$  and  $Z_o$ , respectively, and their effective impedances seen from the antenna terminals are represented by  $Z'_s$  and  $Z'_o$  as illustrated in Fig. 15. It was evident that, since  $AF'_1$  and  $AF'_2$  depend on  $Z'_s$  and  $Z'_o$ , respectively, the SSM yields an antenna factor related to the effective load impedance presented by the cables and associated devices. Therefore, an additional conversion was found necessary to determine the desired antenna factor, which depends on the actual load of each antenna,  $Z_s$  or  $Z_o$ . In addition, it was found that the existing method specified in ANSI C63.5 is not applicable to antennas having height-dependent antenna factors, because it requires a height scan of the receiving antenna. To improve this method, it was proposed that both transmitting and receiving antennas should be placed at the same height above the ground plane during the site attenuation measurements. In contrast to this, Alexander et al. proposed that the antennas be fixed at a height not the same but specific to each antenna [33]. In conjunction to these improvements, the CISPR has recently been discussing validation procedures for an antenna calibration site which require accurate measurements of site attenuation between two calculable dipole antennas and comparison of the measurement results with the theoretical values [36].



Equation (7) is accurate only when the distance between two antennas is greater than one wavelength. Therefore, Gavenda tried to determine correction factors which were required to make the SSM applicable to near-field site attenuation measurements [37]. The correction factors were calculated by taking account of the effects of the reactive field in the vicinity of the antennas. It was found that the omission of those effects introduces an error of as much as 2.0 dB at 30 MHz. Iida et al. also computed the near-field correction factors by using the induced EMF method, which considered not only the reactive field but also the mutual coupling between antennas [38]. The derived factors were applicable to the measurements using tuned dipole antennas. The correction factors proposed so far were calculated for a specific theoretical model of the antenna under calibration. Sugiura et al. therefore pointed out that it was inappropriate to use any correction factors in antenna calibration, because actual antennas may have different structures, stray impedances, and unknown defects [35].

## 5. Conclusions

Rapid increase of portable telephones and digital equipment have highlighted possible radio interference between them. Hence, urgent development of EMI measurement techniques in the microwave frequency range is requested to control interference. One essential technique is related to accurate measurement of the waveforms of broadband EM disturbances. In addition, statistical measurements of the disturbance waveform are also indispensable for estimating the quality degradation in telecommunications caused by disturbances.

Considering this situation, the present paper reviewed the state of the art of broadband antennas and sensors which can be used in measurement of fast-transient disturbances, such as those generated by ESD. Most antennas were found to employ electrically-short radiating elements and O/E or E/O devices. The time-domain response of these sensors to broadband disturbances can be successfully analyzed using the complex antenna factors.

Recently, the CISPR has been discussing the limits and measurement methods for disturbances radiated from electronic equipment in the frequency range above 1 GHz. Along with this, accurate calibration methods of EMI antennas have been strongly requested by radio regulatory authorities and the electronic industry. Hence, this paper reviewed recent improvements achieved in antenna calibration techniques. Referring to these advanced methods, CISPR has currently conducted intensive studies of the methods for calibrating EMI antennas and for verifying calibration sites.

## References

- [1] H. S. Berger, V. Kumara, and K. Matloubi, "Consideration in the design of a broadband E-field sensing system," Proc. 1988 IEEE Inter. Symposium on EMC, pp. 383-389, Seattle, 1988.
- [2] M. Kanda and L. D. Driver, "An isotropic electric field probe with tapered resistive dipoles for broadband use, 100 kHz-18 GHz," Proc. 1986 IEEE Inter. Symposium on EMC, pp. 256-261, San Diego, 1986.
- [3] T. Schmid, O. Egger, and N. Kuster, "Automated E-field scanning system for dosimetric assessment," IEEE Trans. Microwave Theory & Tech., vol. 44, no. 1, pp. 105-113, 1996.
- [4] M. H. Sun, K. A. Wickersheim, A. Kamal, and W. R. Kolbeck, "Fiberoptic sensor for minimally-perturbing measurement of electric field in high power microwave environments," Proc. 1990 Material Society Meeting in San Francisco, California, 1990.
- [5] T. Kobayashi, T. Nojima, K. Yamada, and S. Uebayashi, "Dry phantom composed of ceramics and its application to SAR estimation," IEEE Trans. Microwave Theory & Tec., vol. 41, no. 1, pp. 136-140, 1993.
- [6] K. Murakawa, N. Kuwabara, and F. Amemiya, "Radiation properties of a spherical dipole antenna," Proc. IEEE International Symposium on EMC, Nagoya, pp. 572-576, 1989.
- [7] B. Archambeault and M. Seth, "A new standard radiator for shielding effectiveness measurements," Proc. IEEE International Symposium on EMC, Anaheim CA, pp. 256-265, 1992.
- [8] R. J. Phelan Jr., D. R. Larson, and P. A. Simpson, "A sensitive, high frequency, electromagnetic field probe using a semiconductor laser in a small loop antenna," SPIE, vol. 566 Fiber Optic and Laser Sensors III, pp. 300-306, 1985.
- [9] A. Daryoush and R. Kunath, "Optically controlled arrays—latest techniques—," Proc. IEEE Antennas and Propagation-Society International Symposium, Ann Arbor, pp. 1530-1534, 1993.
- [10] H. I. Bassen and G. S. Smith, "Electrical field probes—A review," IEEE Trans. Antennas & Propag., vol. AP-31, no. 5, pp. 710-718, Sept. 1983.
- [11] J. C. Wyss and S. T. Sheeran, "A practical optical modulator and link for antenna," IEEE J. Lightwave Technol., vol. LT-3, no. 2, pp. 216-321, 1985.
- [12] V. B. Baglikov, R. Yu. Dolinin, E. M. Pelekhatyi, and R. F. Tavlykaev, "Investigation of an electric field sensor based on an integrated optical Mach-Zehnder modulator," Sov. J. Quantum Electron., vol. 18, no. 10, pp. 1353-1355, 1988.
- [13] Y. Tokano, T. Tanabe, R. Muramatsu, M. Kondo, and Y. Sato, "Highly sensitive optical electric field sensor," IEICE Technical Report, EMCJ94-26, 1994.
- [14] N. Kuwabara and R. Kobayashi, "Development of electric field sensor using Mach-Zehnder interferometer," 11th International Zurich Symposium on EMC, pp. 489-494, 1995.
- [15] K. Tajima, N. Kuwabara, R. Kobayashi, and M. Tokuda, "Evaluation of electric field sensor with very small element using Mach-Zehnder interferometer," IEICE Trans., vol. J79-B-II, no. 11, pp. 744-753, 1996.
- [16] M. Shinagawa and T. Nagatsuma, "An electro-optic probing system for diagnosis of ultra-high speed LSIs," NTT R & D, vol. 41, no. 10, pp. 1211-1220, 1992.
- [17] P. F. Wilson and M. T. Ma, "Field radiated by electros-

- tatic discharges," *IEEE Trans. Electromagn. Compat.*, vol. 33, no. 1, pp. 10-18, 1991.
- [18] R. Heidemann, T. Pfeiffer, and D. Jager, "Optoelectrically pulsed slot-line antennas," *Electron. Lett.*, vol. 19, no. 9, pp. 316-317, 1983.
- [19] K. P. Esselle and S. S. Stuchly, "An electrically large antenna for transient electromagnetic field measurements," *IEEE Trans. Instrum. Meas.*, vol. 40, no. 2, pp. 460-464, 1991.
- [20] K. P. Esselle and S. S. Stuchly, "Pulse-receiving characteristics of resistively loaded dipole antennas," *IEEE Trans. Antennas & Propag.*, vol. 38, no. 10, pp. 1677-1683, 1990.
- [21] C. E. Baum, E. L. Breen, J. C. Giles, J. O'Neill, and G. D. Sower, "Sensors for electromagnetic pulse measurements both inside and away from nuclear sources regions," *IEEE Trans. Electromagn. Compat.*, vol. EMC-20, no. 1, pp. 22-35, 1978.
- [22] T. W. Wiekowski, R. A. Makowski, and J. M. Janukiewicz, "Probes for EMP measurement methods of pulse shape reconstruction," *Internat. Wroclaw Symp. on EMC (EMC'92)*, pp. 461-465, 1992.
- [23] H. -M. Shen, R. W. P. King, and T. T. Wu, "New sensors for measuring very short electromagnetic pulses," *IEEE Trans. Antennas & Propag.*, vol. 38, no. 6, pp. 838-846, 1990.
- [24] R. Middelkoop, "Time-domain calibration of field sensors for electromagnetic pulse (EMP) measurements," *IEEE Trans. Instrum. Meas.*, vol. 40, no. 2, pp. 455-459, 1991.
- [25] M. Kanda, "Transients in a resistively loaded linear antenna compared with those in a conical antenna and TEM horn," *IEEE Trans. Antennas & Propag.*, vol. AP-28, no. 1, pp. 132-136, 1980.
- [26] M. Kanda, "The time-domain characteristics of a traveling-wave linear antenna with linear and nonlinear parallel loads," *IEEE Trans. Antennas & Propag.*, vol. AP-28, no. 2, pp. 267-276, 1980.
- [27] I. Yokoshima, S. Ishigami, A. Sugimoto, and H. Iida, "Measurement of complex antenna factor of monopole antenna," *IEICE Technical Report, EMCJ93-20*, 1993.
- [28] S. Ishigami, R. Gokita, Y. Nishiyama, I. Yokoshima, and T. Iwasaki, "Measurements of fast transient fields in the vicinity of short gap discharges," *IEICE Trans. Commun.*, vol. E78-B, no. 2, pp. 199-260, 1995.
- [29] S. Ishigami and T. Iwasaki, "Evaluation of charge transition in a small gap discharge," *IEICE Trans. Commun.*, vol. E79-B, no. 4, pp. 474-482, 1996.
- [30] M. Kanda, "Methodology for electromagnetic interference measurements," *IEICE Trans. Commun.*, vol. E78-B, no. 2, pp. 88-108, 1995.
- [31] R. G. Fitzgerald, "Standard linear antennas, 30 to 1000 MHz," *IEEE Trans. Antennas & Propag.*, vol. AP-34, no. 12, pp. 1425-1429, 1986.
- [32] M. J. Salter and M. J. Alexander, "EMC antenna calibration and the design of an open-field site," *Meas. Sci. Technol.*, vol. 2, no. 6, pp. 510-519, 1991.
- [33] M. J. Alexander, M. J. Salter, D. G. Gentle, and K. P. Holland, "Advances in measurement methods and reduction of measurement uncertainties associated with antenna calibration," *IEE Proc. -Sci. Meas. Technol.*, vol. 141, no. 4, pp. 283-286, 1994.
- [34] A. A. Smith, Jr., "Standard-site method for determining antenna factors," *IEEE Trans. Electromag. Compat.*, vol. EMC-24, no. 3, pp. 316-322, 1982.
- [35] A. Sugiura, T. Morikawa, K. Koike, and K. Harima, "An improvement to the standard site method for accurate EMI antenna calibration," *IEICE Trans. Commun.*, vol. E78-B, no. 8, pp. 1229-1237, 1995.
- [36] J. J. Geodbloed, "Progress in standardization of CISPR antenna calibration procedures," *Proc. 1995 Int'l Zurich Symp. on EMC*, pp. 111-116, 1995.
- [37] J. D. Gavenda, "Near-field corrections to site attenuation," *IEEE Trans. Electromag. Compat.*, vol. EMC-36, no. 3, pp. 213-220, 1994.
- [38] H. Iida, S. Ishigami, I. Yokoshima, and T. Iwasaki, "Measurement of antenna factor of dipole antennas on a ground plane by 3-Intenna method," *IEICE Trans. Commun.*, vol. E78-B, no. 2, pp. 260-266, 1995.



**Akira Sugiura** was born in Fukui Prefecture, Japan, in 1943. He received the BS degree in applied physics from Fukui University in Japan in 1966 and the MS degree from Osaka University in the same field in 1968. After graduation, he joined the Communications Research Laboratory (formerly the Radio Research Laboratory), Ministry of Posts and Telecommunications. He has since been engaged in studies of EMC measurements

and antenna calibration. In 1996 he received the Dr. Eng. degree from Tokyo Institute of Technology. He is currently Director of the Electromagnetic Technology Division of the CRL. He is a member of IEEE.



**Nobuo Kuwabara** received the B.E. and M.E. degrees in Electrical Engineering from Shizuoka University, Shizuoka, Japan, in 1974 and 1976, respectively, and the Dr.Eng. degree from Shizuoka University in 1992. Since joining NTT in 1977, he has been engaged in research on the overvoltage protection of telecommunications system and the design of the induction free optical fiber cable. He is currently involved in studies of the electromagnetic compatibility on telecommunication system. He is a manager of electromagnetic environment research group in NTT Multimedia Networks Laboratories. Dr. Kuwabara is a member of the IEEE.